CENTER FOR COMPUTATIONAL MATHEMATICS REPORTS

University of Colorado at Denver
P.O. Box 173364, Campus Box 170
Denver, CO 80217-3364

Fax: (303) 556-8550
Phone: (303) 556-8442
http://www-math.cudenver.edu/

February 1996 UCD/CCM Report No. 74

Upscaling of Dispersivity in Modeling of Solute Transport: Mathematical Theory and Laboratory Experiments

T.F. Russell, D.W. Dean, T.H. Illangasekare,
R. Mapa and J. Garcia

In: Proceedings of the International Conference on Modeling of Flows in Porous Media, Université Jean Monnet, St.-Étienne, France, 1996.

Upscaling of Dispersivity in Modeling of Solute Transport: Mathematical Theory and Laboratory Experiments

T. F. Russell and D. W. Dean
University of Colorado at Denver, Denver, CO 80217-3364, U.S.A.

T. H. Illangasekare, R. Mapa, and J. Garcia
University of Colorado at Boulder, Boulder, CO 80309-0428, U.S.A.

Introduction

Groundwater modeling for environmental restoration is of major and growing concern. Heterogeneities in fluids and subsurface formations control to a large extent the effectiveness of remediation technologies in the field. These variations exist over a wide range of length scales, from the size of pores to regional scales (e.g., [18]).

Process understanding at a small scale does not necessarily lead in a straightforward manner to appropriate models at a larger scale. Indeed, the form of the governing equations may be entirely different, as in the passage from Navier-Stokes equations at the pore level to Darcy's law at laboratory and larger scales [17]. In practical modeling, the goal is to compute numerically with models that are valid at the scale of the computational grid. Subgrid heterogeneities cannot be represented directly by simulator data, and must be reflected in the choice of governing equations and in the manner in which laboratory data are scaled up for use in these field-scale equations. Ideally, we would like to have scaling rules that would tell us the form of the equations and the values of grid-scale coefficients.

Upscaling in porous media is a long-term problem requiring interdisciplinary theoretical, computational, and experimental research. Theory provides a framework within which to set up computations and experiments, and an ultimate goal of research in this area is a theoretical methodology for derivation of upscaled models. The models are intended for practical grid-scale computations, necessitating understanding of model behavior in the context of numerical approximation errors on a range of scales. Experiments test the range of validity of theories and the accuracy and appropriateness of computational approaches, yielding the physical benchmarks that scaling methodologies must attempt to match. The present paper documents work in progress on this variety of fronts in the context of dispersivity in passive solute transport, where a time-independent velocity field is obtained from a flow equation.

In discussions of upscaling, one usually thinks first of (single-phase) flow, where a primary concern is averaging of formation properties (in particular, hydraulic conductivity) to the scale of grid cells. This leads to forms such as a full-tensor conductivity, even if principal flow directions are aligned with grid coordinates so that the local sub-grid conductivity is an anisotropic diagonal tensor. This has been studied extensively by many investigators [19, 24, 11] and, while of vital importance, is not the focus of the present study. What is important in our context is the existence of a relationship between the Fourier transforms of velocity covariances and of log-hydraulic conductivity covariances (e.g., [5]), based on spectral arguments [14, 21]. Hence, estimates of dispersivity can be based on either velocity covariances or conductivity covariances. Our present thinking is that numerical procedures

can be more effectively formulated if conductivity covariances are used, and this is what is outlined below.

The remainder of this paper discusses the philosophy behind the authors' approach to upscaling, describes a numerical Lagrangian stochastic method under development, and outlines the first related experimental results. This should be regarded as a tentative preliminary stage of a long-term effort.

Philosophy

A major reason for the lack of solid understanding of scaling of transport in heterogeneous media is that theoretical models tend to be idealized, making assumptions or addressing limiting cases that are not representative of real formations. While differences exist in specifics, it is widely accepted that subsurface porous media in the field exhibit a discrete hierarchy of scales. For example, Haldorsen [18] speaks of four scales: microscopic (pores and sand grains), macroscopic (core plug), megascopic (layers, fractures, faults, field-scale simulation grids), and gigascopic (formation, basin, regional). Each has its own effects on flow, distinct from the others. The present research seeks to move toward such less-idealized models. To do this, it is important to understand the idealized approaches, the contributions they may make to practical models, and their limitations. The idealizations known to the authors can be broadly classified into homogenization, stochastics, and fractals.

The framework for homogenization involves short and long length scales, λ and Λ respectively, with the ratio $\epsilon = \lambda/\Lambda$ as a small parameter. There are two approaches, volume averaging [23] and perturbation expansions in ϵ [12], which are essentially equivalent [1]. An effective large-scale model is obtained from a periodic small-scale one as the small parameter ϵ is taken to 0. Generally, the coefficients in the large-scale model are not determined explicitly, but are themselves solutions of partial differential equations.

Several questions suggest themselves regarding the practicality of applications. Instead of two scales whose ratio can be viewed as a small parameter, one expects to be concerned with multiple scales whose ratios have finite pre-asymptotic values. It is natural to ask what homogenization theory will yield when ϵ is finite, expecting that the result will be non-local in space (small-scale variations make a finite contribution at the large scale and cannot be completely averaged out), and whether it is feasible to iterate the two-scale theory over a greater number of scales. With finite ϵ, the question of the sensitivity of the theoretical model to the value of this parameter poses itself. In addition, the theory becomes quite complicated as even relatively simple physics is introduced into the small-scale governing equations, and the feasibility of extending the theory to more complex physical processes is an issue, although the theory, in the asymptotic limit, already deals with the process of passive solute transport addressed in this work [23]. Finally, for practical purposes the homogenized coefficients must be computable, so the matter of the computational complexity of the partial differential equations for them must be considered.

Traditional stochastic methods generally assume that the logarithm of hydraulic conductivity and the velocity are stationary random fields, with mean-zero perturbations that have exponentially decaying autocorrelation, and that the conductivity has small variance and the velocity is a small perturbation of a uniform flow. The scales involved in these methods are

a transport scale L and a statistical correlation scale λ, where the autocorrelation between perturbations at locations $\vec{X}$ and $\vec{X}+\vec{r}$ separated by a vector $\vec{r}$ of magnitude r is $e^{-r/\lambda}$. The correlation scale may be anisotropic, i.e., different scales $\lambda_x, \lambda_y, \lambda_z$ may apply in different directions. The theories (e.g., [14, 3, 21]) derive effective dispersivities as L/λ tends to infinity, i.e., as the transport becomes ergodic, so that the average behavior of an ensemble of realizations of the stochastic process represents the behavior of a single realization.

In contrast to traditional stochastic approaches, which assume a single correlation scale, fractal models postulate that porous media exhibit self-similarity through all, or a wide range of, scales [27]. That is, the view of the porous medium from the perspective of one particular scale is the same as that from any other. Instead of an exponentially decaying autocorrelation, this leads to a power law of the form r^{-b} [15, 28]. From this point of view, it becomes necessary to measure properties experimentally on a variety of scales in order to calibrate the fractal behavior and fit the theoretical model [27].

In analogy with the finite ϵ for homogenization, one must ask what stochastic methods yield for a pre-ergodic ratio L/λ of transport scale to correlation scale. Indications are that the result will be a non-local theory in which dispersivity will depend on memory as well as the current state of the system [2, 8], leading to an integrodifferential equation. Questions of feasibility and computability then naturally arise.

Additionally, one must also acknowledge that real multi-scale media lie somewhere between the single-correlation-scale stochastic and continuous-scale fractal idealizations. Variations of field dispersivity data from fractal self-similarity have been attributed to approximate stationarity of discrete geological units on a hierarchy of scales [22]. A model with a finite number of discrete correlation scales and some form of superposition seems to be indicated. Reasonable ideas along these lines can be suggested, but we do not discuss details here.

A central theme of practical models must be an attempt to account for the non-asymptotic nature of real media. That is, to the extent possible, the concepts must be adapted to non-ideal cases in which a parameter, which tends to zero or infinity in the idealizations, takes a finite value instead. We wish to avoid assumptions of ergodicity, periodicity, small variance, near-uniform flow, and single or continuous correlation scale. This appears to dictate a numerical approach, meaning that we should operate in a theoretical framework that is suitable for computation with accurate numerical methods and is extendible to complex problems.

Lagrangian Stochastic Dispersion Model

The authors' view is that the best hope for such a numerical approach is a flexible stochastic framework, computing with media whose properties exhibit the desired non-ideal correlation structure. In particular, Dagan [7, 8] has presented a Lagrangian-based formulation that can lead to specification of the dispersivity tensor at the level of numerical grid blocks. The Lagrangian frame meshes well with numerical techniques studied by the first author for many years (e.g., [10, 25]). Our model that parallels and extends this formulation will be outlined here; details will appear elsewhere [9].

We begin with the deterministic solute mass transport equation

$$\frac{\partial c}{\partial t} + \vec{V} \cdot \nabla c = \nabla \cdot (\mathbf{D} \nabla c), \tag{1}$$

where $c(\vec{X}, t)$ is solute concentration, $\mathbf{D}$ represents the dispersivity tensor, and $\vec{V}$ is the seepage velocity

$$\vec{V} = -\frac{\mathbf{K}}{n} \nabla \phi, \tag{2}$$

where $\mathbf{K}$ is the hydraulic conductivity, n is the porosity and ϕ is the hydraulic head. We have the total mass (0^{th} moment)

$$M_0(t) = \int_\Omega n c(\vec{X}, t) d\vec{X}, \tag{3}$$

the first moment and centroid (vectors)

$$\vec{M}_1(t) = \int_\Omega n \vec{X} c(\vec{X}, t) d\vec{X}, \qquad \vec{R}(t) = \frac{\vec{M}_1}{M_0}, \tag{4}$$

and the second moment (tensor entries) about the centroid

$$\mathbf{M_2}_{ij}(t) = \int_\Omega n (X_i - R_i(t))(X_j - R_j(t)) c(\vec{X}, t) d\vec{X}. \tag{5}$$

Routine calculations then show that the entries of the dispersivity tensor are

$$\mathbf{D}_{ij}(t) = \frac{1}{2} \frac{d}{dt} \left[\frac{\mathbf{M_2}_{ij}(t)}{M_0(t)} \right] \equiv \frac{1}{2} \frac{d}{dt} \left[\mathbf{S}_{ij}(t) \right]. \tag{6}$$

Now we consider stochastic transport, where expectations $\mathbf{E}$ are defined by integration over the random variable ω, which is suppressed in the notation. In the Lagrangian framework, transport is developed in terms of indivisible solute particles that are convected by the fluid. The velocity covariances are defined as

$$\vec{V}' = \vec{V} - \mathbf{E}[\vec{V}], \tag{7}$$

$$\rho_{ij}(\vec{x}, \vec{y}) = \mathbf{E}[\vec{V}'_i(\vec{x}) \vec{V}'_j(\vec{y})], \tag{8}$$

where $\vec{V}'$ is the particle's deviation from the ensemble expectation. If the vector $\vec{X}_T$ represents the total displacement of the particle which started its motion at $\vec{x} = \vec{x_0}$, $t = 0$, then the vector $\vec{X}_T$ can be decomposed into

$$\underbrace{\vec{X}_T(t; \vec{x_0}, 0)}_{Total\ Displacement} = \underbrace{\vec{X}(t; \vec{x_0}, 0)}_{Convection} + \underbrace{\vec{X}_d(t; 0)}_{Diffusion}. \tag{9}$$

Here $\vec{X}_d$ is the integral of a white noise process. The vector $\vec{X}$ comes from convective transport; assuming near-uniform flow, so that $\mathbf{E}[\vec{V}]$ is time-independent, Dagan [3] obtains for the fluctuation $\vec{X}' \equiv \vec{X} - \mathbf{E}[\vec{X}]$ that

$$\begin{aligned} \vec{X}'(t; \vec{x_0}, 0) &= \vec{X}(t; \vec{x_0}, 0) - \mathbf{E}[\vec{V}] t \\ &= \int_0^t \vec{V}'(\mathbf{E}[\vec{V}] t') dt'. \end{aligned} \tag{10}$$

Based on (10), the displacement covariance tensor entries $\mathbf{X}_{ij}$ are then expressed in terms of the velocity covariances in (8) as

$$\begin{aligned}\mathbf{X}_{ij}(t;\vec{x_0},0) &= \mathbf{E}[X'_i(t;\vec{x_0},0)X'_j(t;\vec{x_0},0)] \\ &= \int_0^t \int_0^t \rho_{ij}(\mathbf{E}[\vec{V}]t', \mathbf{E}[\vec{V}]t'')dt'dt''. \end{aligned} \tag{11}$$

These are important because of the fundamental relationship [6], noting that $\mathbf{S}_{ij}$ is now a random variable,

$$\mathbf{D}_{ij} = \frac{1}{2}\frac{d\mathbf{E}[\mathbf{S}_{ij}]}{dt} = \frac{1}{2}\frac{d\mathbf{X}_{ij}}{dt} - \frac{1}{2}\frac{d\mathbf{R}_{ij}}{dt}, \tag{12}$$

where $\mathbf{R}_{ij}$ is the analogue of $\mathbf{X}_{ij}$ for the centroid position vector $\vec{R}$. Here $\mathbf{D}_{ij}$ is deterministic and represents the expected dispersivity of a single realization due to velocity variations; the $\mathbf{X}$ term in (12) is the dispersivity of the ensemble-average concentration, which is larger because it includes spreading due to the uncertainty of the centroid location over multiple realizations.

Note the time integrals in (11). These are advantageous in numerical computations of $\mathbf{D}_{ij}$, because they allow $d\mathbf{X}_{ij}/dt$ to be evaluated without error-prone differentiation. We outline here a numerical approach, based on conductivity covariances, that preserves this property and does not require an assumption of near-uniform flow. A key benefit of the numerical viewpoint is that we can make use of *local* assumptions. Here, during one time step, we assume that the seepage velocity for a given fluid particle in a given realization is constant in time. No such assumption is made on a *global* basis. In a similar vein, we assume that the hydraulic gradient-porosity quotient $\nabla\phi/n$ is locally constant and locally deterministic (since we are interested in the statistics of $\mathbf{K}$ and $\vec{V}$).

Let $[0,t]$ be a time step and let $\vec{r}$ be the position vector at time t of a fluid particle that originates at $\vec{r_0}$ at time 0 (to simplify notation, let $\vec{r_0} = 0$). This vector is given by the kinematic relationship

$$\vec{r} = \int_0^t \vec{V}(t')dt' = -\int_0^t \frac{\mathbf{K}}{n}\nabla\phi dt' \tag{13}$$

The deviation of the position vector $\vec{r}$ from its expected value is given by $\vec{r} - E[\vec{r}]$, and the matrix of covariances of these deviations is given by the following analogue of (11):

$$\begin{aligned}\mathbf{X} &= \mathbf{E}\left[(\vec{r} - \mathbf{E}[\vec{r}])(\vec{r} - \mathbf{E}[\vec{r}])^T\right] \\ &= \mathbf{E}\left[\left(\int_0^t \frac{\mathbf{K}}{n}\nabla\phi dt' - \mathbf{E}\left[\int_0^t \frac{\mathbf{K}}{n}\nabla\phi dt'\right]\right)\left(\int_0^t \frac{\mathbf{K}}{n}\nabla\phi dt' - \mathbf{E}\left[\int_0^t \frac{\mathbf{K}}{n}\nabla\phi dt'\right]\right)^T\right] \\ &= \mathbf{E}\left[\left\{\mathbf{K}'\frac{t\nabla\phi}{n}\right\}\left\{\mathbf{K}'\frac{t\nabla\phi}{n}\right\}^T\right], \end{aligned} \tag{14}$$

where $\mathbf{K}' = \mathbf{K} - \mathbf{E}[\mathbf{K}]$, assuming that $\mathbf{K}'$ is locally constant. Since

$$\mathbf{E}[\vec{r}] = t\mathbf{E}[\vec{V}] = \frac{t}{n}\mathbf{E}[\mathbf{K}]\nabla\phi, \tag{15}$$

we obtain

$$\mathbf{X} = \mathbf{E}\left[\left(\hat{\mathbf{K}}\mathbf{E}[\vec{r}]\right)\left(\hat{\mathbf{K}}\mathbf{E}[\vec{r}]\right)^T\right], \tag{16}$$

where $\hat{\mathbf{K}} = \mathbf{K}'\mathbf{E}[\mathbf{K}]^{-1} = \mathbf{K}\mathbf{E}[\mathbf{K}]^{-1} - \mathbf{I}$. For m space dimensions, some tedious algebra leads to

$$\frac{1}{2}\frac{d\mathbf{X}_{ij}}{dt} = \frac{1}{2}\sum_{k=1}^{m}\mathbf{E}\left\{\sum_{\ell=1}^{m}(\hat{\mathbf{K}}_{ik}\hat{\mathbf{K}}_{j\ell} + \hat{\mathbf{K}}_{i\ell}\hat{\mathbf{K}}_{jk})\mathbf{E}[r_\ell]\right\}\mathbf{E}[V_k]. \tag{17}$$

If $\mathbf{K}$ is diagonal and if $\mathbf{E}[\vec{r}]$ is approximated locally in time by $\mathbf{E}[\vec{V}]t$, then (17) reduces to

$$\frac{1}{2}\frac{d\mathbf{X}_{ij}}{dt} = \mathbf{E}[\hat{\mathbf{K}}_{ii}\hat{\mathbf{K}}_{jj}]\mathbf{E}[V_i]\mathbf{E}[V_j]t. \tag{18}$$

The expected velocity in (17)–(18) varies from grid block to grid block. Over time, a Lagrangian particle will pass through various blocks, accumulating local contributions of the type outlined above. Suppose that the trajectory $\vec{X}_T$ spends from t_0 to t_1 on grid block 1, from t_1 to t_2 on grid block 2, and so on to grid block n. On this time-step basis, assume locally that $\nabla\phi$ does not depend on time and the statistics of $\mathbf{K}$ do not depend on time on individual grid blocks. Then

$$\vec{r} = -\sum_{k=0}^{n-1}\int_{t_k}^{t_{k+1}}\frac{\mathbf{K}^{(k+1)}}{n}\nabla\phi^{(k+1)}dt' = -\sum_{k=0}^{n-1}\int_{t_k}^{t_{k+1}}\mathbf{K}^{(k+1)}dt'\,\frac{\nabla\phi^{(k+1)}}{n}, \tag{19}$$

$$\mathbf{E}[\vec{r}] = -\sum_{k=0}^{n-1}\int_{t_k}^{t_{k+1}}\mathbf{E}[\mathbf{K}^{(k+1)}]dt'\,\frac{\nabla\phi^{(k+1)}}{n}, \tag{20}$$

$$\vec{r} - \mathbf{E}[\vec{r}] = -\sum_{k=0}^{n-1}\int_{t_k}^{t_{k+1}}\mathbf{K}'^{(k+1)}dt'\,\frac{\nabla\phi^{(k+1)}}{n}. \tag{21}$$

Proceeding as in (14)–(16), we obtain

$$\begin{aligned}\mathbf{X} &= \mathbf{E}\left[(\vec{r} - \mathbf{E}[\vec{r}])(\vec{r} - \mathbf{E}[\vec{r}])^T\right] \\ &= \sum_{k=0}^{n-1}\sum_{\ell=0}^{n-1}\mathbf{E}\left[\hat{\mathbf{K}}^{(k+1)}\mathbf{E}[\vec{r}^{(k+1)}]\hat{\mathbf{K}}^{(\ell+1)}\mathbf{E}[\vec{r}^{(\ell+1)}]^T\right].\end{aligned} \tag{22}$$

Then a representation of $1/2\, d\mathbf{X}_{ij}/dt$ can be developed as above in (17)–(18). The non-local nature of the resulting dispersivity is evident from the temporal summations in (22). To estimate the dispersivity in a given grid block at a given time, ensembles of particles are tracked, indicating those grid blocks that are most likely to contribute to the accumulation. This information also enables the $\mathbf{R}$ term of (12), formulated in a manner similar to the $\mathbf{X}$ term, to be estimated. Upscaling of hydraulic conductivity (e.g., [19, 24, 11]) to grid scale can be incorporated directly into the values of $\mathbf{K}$ used above.

At this writing, the dispersivity calculation procedure has been implemented and tested for the experimental data to be reported below. Preliminary upscaled simulations are in what could be judged to be reasonable agreement with experiment, but it is not appropriate to draw conclusions from this. The experiment represents one realization of a stochastic medium, while upscaled simulations should reproduce averaged behavior of an ensemble of

realizations. To compare the type of simulation outlined above, which predicts expected values of concentration, with experiment, a large number of realizations would need to be used in the laboratory.

Appropriate comparisons with a small number of realizations would be possible, if in addition to expected concentrations we had computations of confidence intervals. To obtain this information about the probability density, it would be desirable to solve a system for the higher-order moments of the concentration, up to second-order. Graham and McLaughlin [16] proposed such a system derived from a method of distributed parameters, under the assumptions of Gelhar and Axness [14] (ergodicity, near-uniform flow, single correlation scale). This work also effectively assumed that concentration and velocity fluctuations formed a multivariate Gaussian distribution, allowing some product terms to be discarded. We are developing algorithms [9], not yet implemented, based on the theory of stochastic differential equations. We intend for these methods to avoid the above assumptions, in particular retaining the product terms. The system involves covariance information for velocities (from conductivities) as well as concentrations, so Monte Carlo solution of the flow equation will be needed.

Laboratory Experiments

The theoretical framework described above is designed to be compared to heterogeneous flow and solute transport experiments with a modest number, yet to be determined, of realizations. The experimental facility, located in the laboratories of the Department of Civil and Environmental Engineering at the University of Colorado at Boulder, is a horizontal soil tank of dimensions 8 ft $\times$ 4 ft (244 cm $\times$ 122 cm). Soil samples of approximately 7 cm thickness can be packed into the tank. Pressure and solute concentration measurements can be taken at the 45 port locations, drilled through the top of the tank, depicted by dots in Figure 1 (more ports were added for some experiments, as described for some examples below), and velocity vectors can be measured at the ports via dye experiments. As this is written, the authors have packed the tank once with homogeneous sand, performing 10 experiments (3 flow only, 7 flow and tracer transport), and again with one heterogeneous realization using 5 different sands in 200 cells of 4.8 in $\times$ 4.8 in (12.2 cm $\times$ 12.2 cm), performing 5 experiments (1 flow, 4 flow and transport). The configuration of the sands is shown in Figure 2. The experiments are reported in full detail, with citations of relevant background literature, by Garcia [13]; here we merely outline the work and present some representative examples.

The top of the tank is a plexiglass plate of thickness 3/4 in (1.91 cm). To assure good contact between the sand and the top wall, preventing bulging of the plexiglass under water pressure, the plexiglass was pushed down by 36 3 in $\times$ 3 in pressure plates spread across the tank. It is known that the porosity of a porous medium along a smooth wall is greater than within the medium; to minimize this effect, which decays with distance from the wall, a minimum width of 2 in (5.08 cm) is needed [26]. In the packing procedure, the tank was divided into 6 (for homogeneous) or 200 (for heterogeneous) compartments by thin metal sheets of height 2.5 in (6.35 cm). The compartments were filled with dry sand, the metal sheets were removed, the plexiglass top was lowered, and the tank was vibrated by hammering

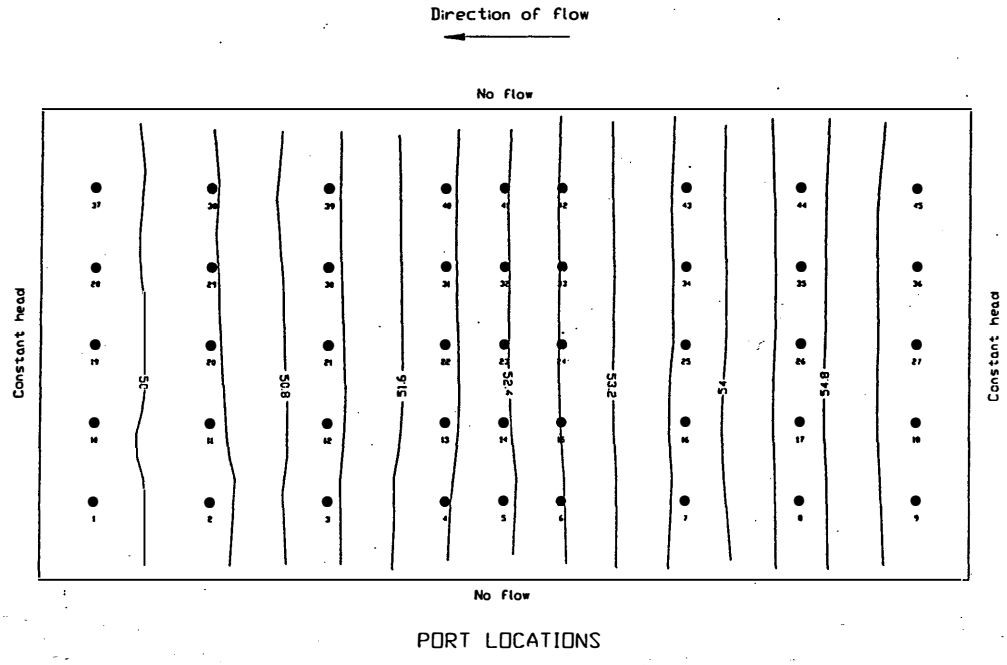

Figure 1. Head contours, homogeneous packing

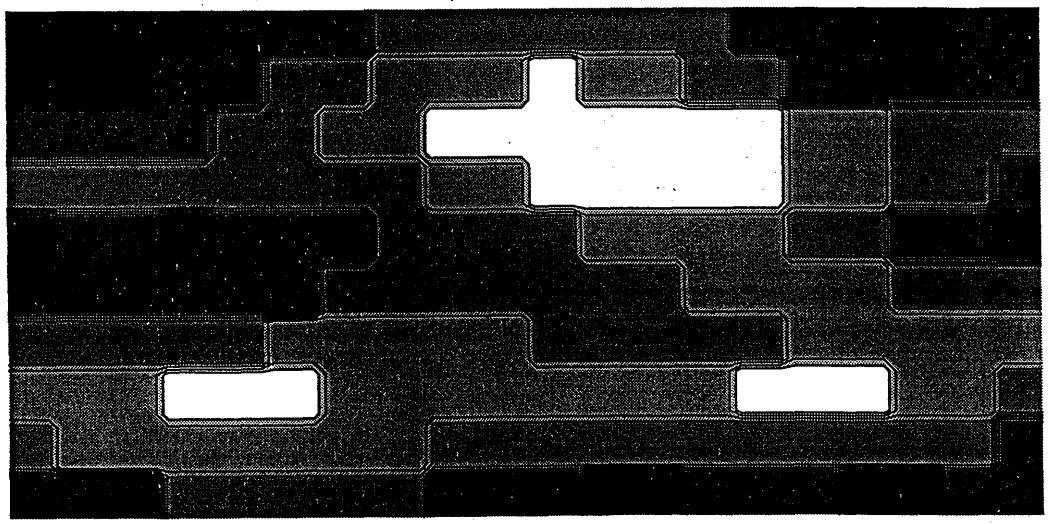

Figure 2. Distribution of 5 heterogeneous sands
(Conductivities: light = high, dark = low)

the bottom aluminum sheet (thickness 1/2 in (1.27 cm)) to achieve uniform settling. After the tank was sealed, a vacuum was applied, carbon dioxide was diffused into the tank, and finally the sand was saturated with de-aired/distilled water.

The sands used in the heterogeneous packing were crushed silica, grades 110, 70, 30, 16, and 8 (Unimin Corp., Emmet, ID). The characterization of these sands is given by Mapa *et al.* [20]. The saturated hydraulic conductivities were measured with a flow cell and found to be, respectively, 0.00425, 0.0135, 0.116, 0.430, and 1.20 cm/sec. Grade 30, the middle sand of conductivity 0.116 cm/sec, was used in the homogeneous experiments.

In all of the experiments, constant-head boundary conditions at the two 4-ft ends of the tank were created by two constant-head end tanks. Water entered and left the main tank through gravel layers at both ends about 4 cm wide. No-flow conditions held on the two 8-ft sides. Experimental data were taken after a flow regime reached steady state. Heads, generally in the range of 20 to 100 cm, were measured by a pressure scanning system that showed an accuracy of ± 0.2 cm when compared with constant-head devices. Tracer injection rates were monitored via the mass outflow from the source reservoir, taking readings every 10 sec with an accuracy of ± 0.1 g. Benzene was used as the tracer in most cases, including the ones shown below, because its concentration could be measured by gas chromatography from a small (2 μl) sample that did not affect pressures in the tank.

The heterogeneous packing was designed to simulate a log-normal distribution of hydraulic conductivity. The five sands appeared in, respectively, 8.5, 21.5, 34.5, 25.5, and 10.0 percent of the 200 cells. The variance of ln $\mathbf{K}$ was 2.86, and fitting the experimental variogram with a negative exponential model yielded longitudinal and transverse correlation lengths $\lambda_\ell = 59.1$ cm (4.85 cell widths) and $\lambda_t = 27.8$ cm (2.28 cell widths).

The figures depict some of the experimental results. The head contours (cm) in Figure 1 show that the hydraulic conductivity in the homogeneous experiments was indeed reasonably uniform. The overall effective hydraulic conductivity was back-calculated in each of the homogeneous experiments from the hydraulic gradient (obtained from the difference in pressure between the first and last column of ports in Figure 1) and the discharge. For the 7 tracer experiments, these results were 0.1474, 0.1654, 0.1669, 0.1747, 0.1776, 0.1785, and 0.1814 cm/sec, compared with the value of 0.116 cm/sec measured in the flow cell. One of these experiments, in which tracer was injected at port 16 and samples were taken downstream at ports 15, 14, and 13, is represented in Figure 3. Benzene was injected at a rate of 5 ml/min for 4 hours. Other experiments took samples at different locations, analyzed experimental errors, and studied breakthrough at the outflow end of the tank. The finite difference models MODFLOW and MT3D were used to determine dispersivities that best matched the breakthrough curves [13]. For the curves in Figure 3, $\alpha_\ell = 0.81$ cm and $\alpha_t/\alpha_\ell = 0.075$ were found.

Figure 4 shows head contours for the heterogeneous packing, now based on measurements at 69 ports. Figure 5 represents velocity vectors measured at these ports, except for the first two columns and the last column, based on dye experiments. The directions of the vectors can be seen to be in good agreement with the normals to the contours. The region of highest conductivity corresponds to the widest spread in head contours, as one would expect. Finally, in Figure 6 we show a streamline predicted by the dye experiments, inject benzene at 4.27 cc/min for 2 hours from port 34-F (in a circle of 8 additional ports of radius 2 in around port 34), and sample concentrations at downstream locations. Other experiments similar

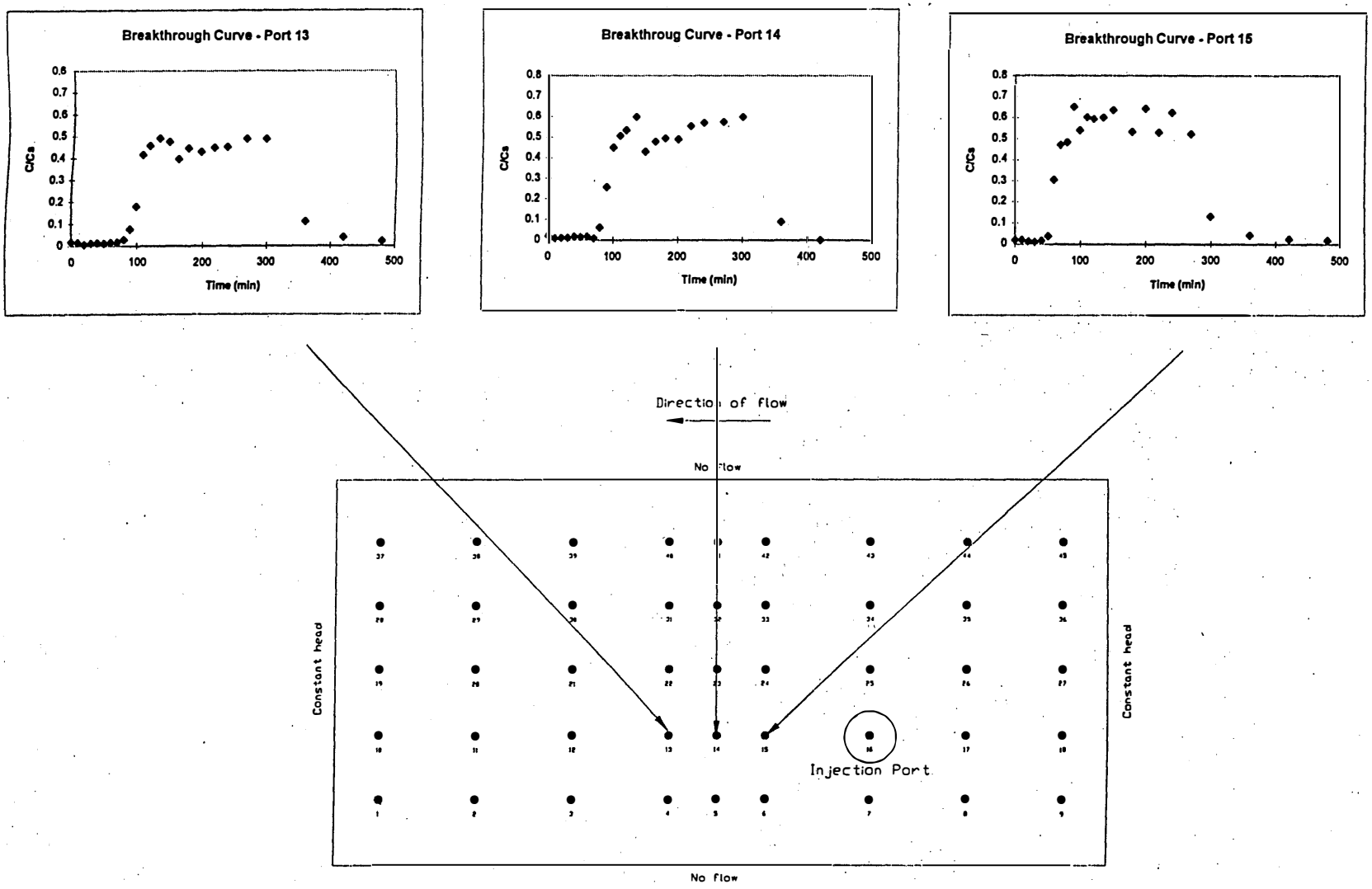

Figure 3. Breakthrough curves, homogeneous packing

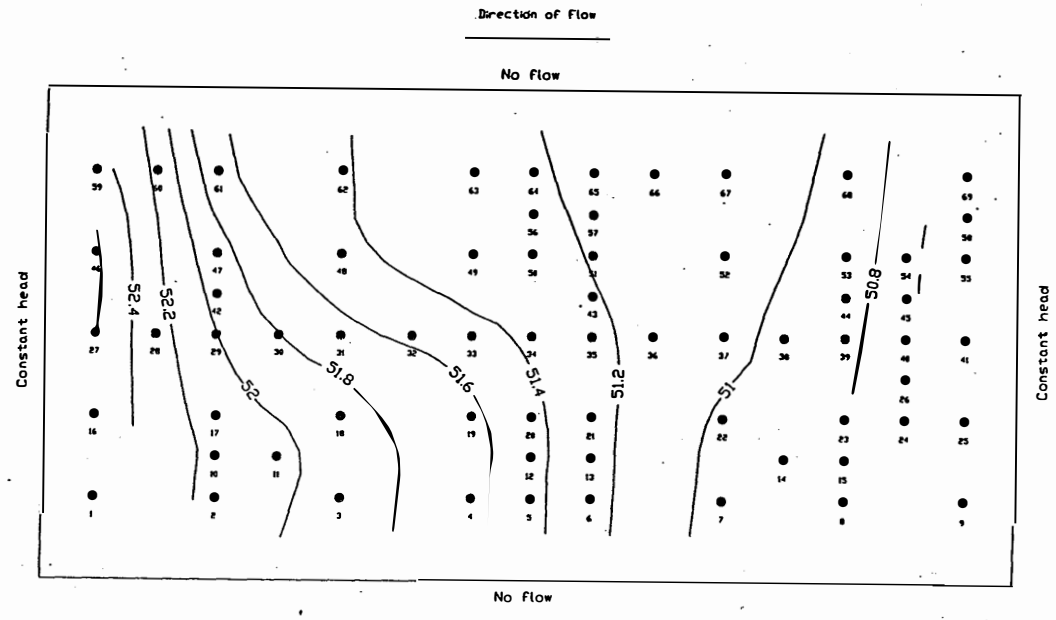

Figure 4. Head contours, heterogeneous packing

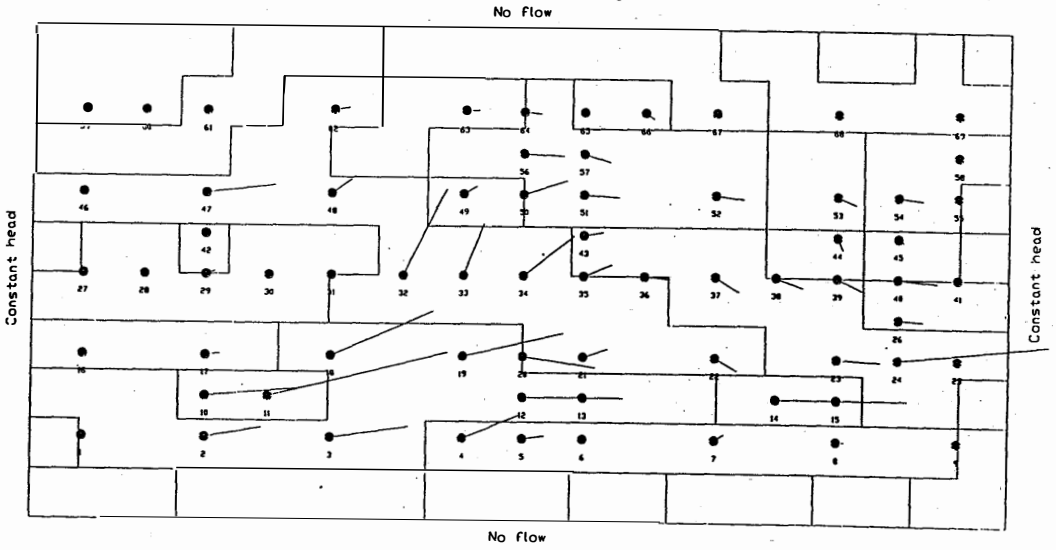

Figure 5. Velocity vectors, heterogeneous packing

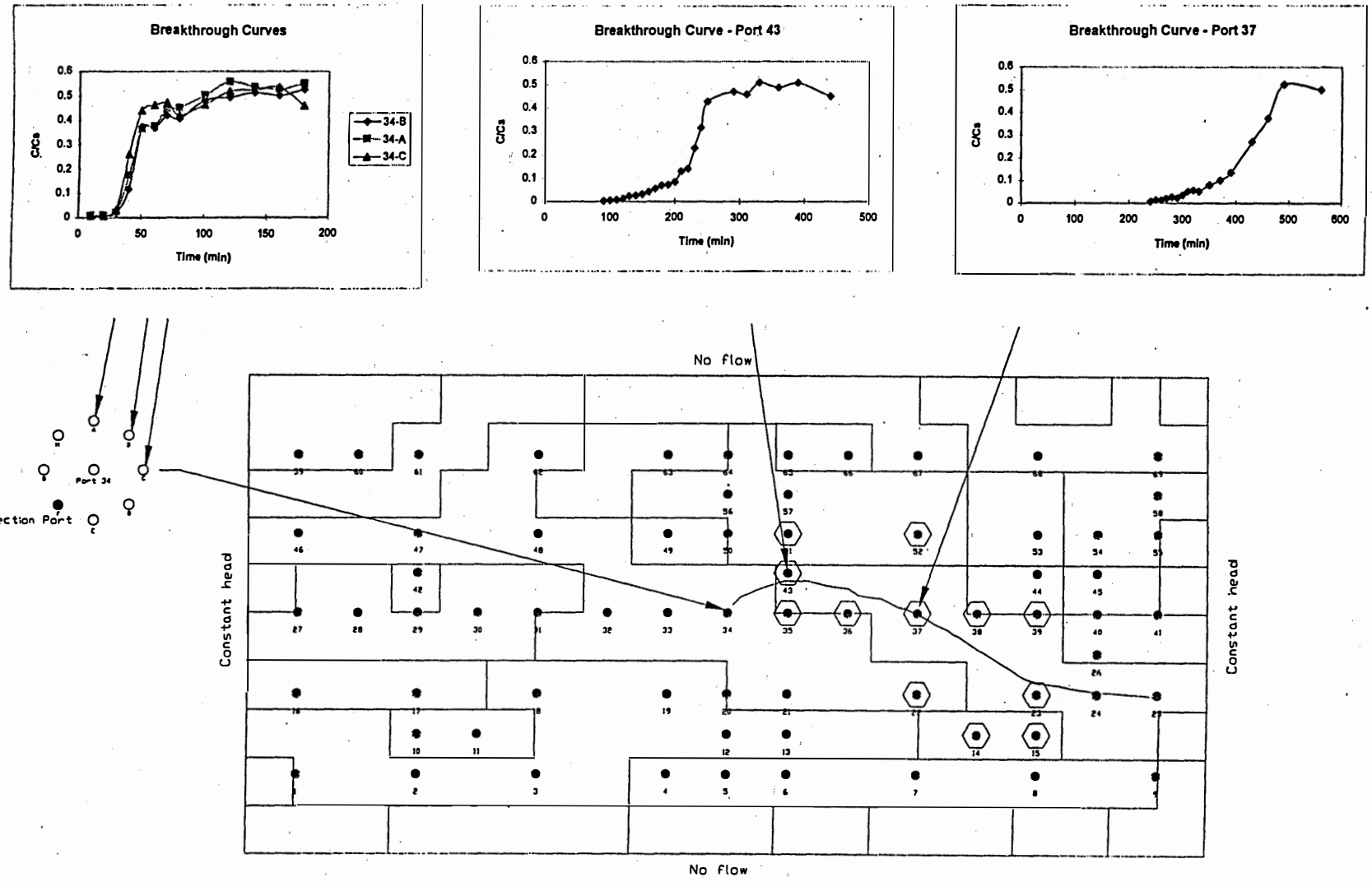

Figure 6. Breakthrough curves, heterogeneous packing

to the homogeneous case were performed, including a bromide tracer across the entire tank that enabled back-calculation of an effective $\alpha_\ell = 43$ cm compared to 61 cm predicted by the theory of Gelhar and Axness [14]. Details are presented by Garcia [13]. These results demonstrate the usefulness of the experimental facility and of the data set, which can begin to test and validate scaling theories and numerical codes.

Acknowledgments

This work was supported by the U.S. Army Waterways Experiment Station. The authors thank J. Holland, S. Howington, J. Peters, and J. Schmidt for many stimulating discussions, and S. Howington for designing the conductivity field for the heterogeneous experiments.

References

[1] Bourgeat, A., Quintard, M., and Whitaker, S., "Éléments de Comparaison entre la Méthode d'Homogénisation et la Méthode de Prise de Moyenne avec Fermature," *C. R. Acad. Sci. Paris, t. 306, Série II* (1988), 463–466.

[2] Cushman, J. H., "Generalized Hydrodynamics of Microporous Media: Relationships between the Memory Function and the Scale of Observation," *Dynamics of Fluids in Hierarchical Porous Media*, J. H. Cushman, ed., Academic Press, London, 1990, pp. 485–499.

[3] Dagan, G., "Solute Transport in Heterogeneous Porous Formations," *J. Fluid Mech., 145* (1984), 151–177.

[4] Dagan, G., "Statistical Theory of Groundwater Flow and Transport: Pore to Laboratory, Laboratory to Formation and Formation to Regional Scale," *Water Resour. Res., 22* (1986), 120S–135S.

[5] Dagan, G., "Theory of Solute Transport by Groundwater," *Ann. Rev. Fluid Mech., 19* (1987), 183–215.

[6] Dagan, G., *Flow and Transport in Porous Formations,* Springer-Verlag, Berlin, 1989.

[7] Dagan, G., "Dispersion of a Passive Solute in Non-Ergodic Transport by Steady Velocity Fields in Heterogeneous Formations," *J. Fluid Mech., 233* (1991), 197–210.

[8] Dagan, G., "Upscaling of Dispersion Coefficients in Transport through Heterogeneous Formations," prepared for the Geostatistics Expert Group Meeting, Sandia National Laboratory, 1993.

[9] Dean, D. W., "Invesigation of Mathematical Modeling of Groundwater Flow and Contaminant Transport: Scale Up, Mathematical Theory and Experimental Validation," Ph.D. Thesis, University of Colorado at Denver, in preparation, 1995.

[10] Douglas, J., Jr., and Russell, T. F., "Numerical Methods for Convection-Dominated Diffusion Problems Based on Combining the Method of Characteristics with Finite Element or Finite Difference Procedures," *SIAM J. Numer. Anal., 19* (1982), 871–885.

[11] Durlofsky, L. J., "Numerical Calculation of Equivalent Grid Block Permeability Tensors for Heterogeneous Porous Media," *Water Resour. Res., 27* (1991), 699–708.

[12] Ene, H. I., "Application of the Homogenization Method to Transport in Porous Media," *Dynamics of Fluids in Hierarchical Porous Media*, J. H. Cushman, ed., Academic Press, London, 1990, pp. 223–241.

[13] Garcia, J., "An Experimental Investigation of Upscaling of Water Flow and Solute Transport in Saturated Porous Media," M.S. Thesis, University of Colorado at Boulder, 1995.

[14] Gelhar, L.W., and Axness, C.L., "Three-Dimensional Stochastic Analysis of Macrodispersion in Aquifers," *Water Resour. Res., 19* (1983), 161–180.

[15] Glimm, J., and Sharp, D. H., "A Random Field Model for Anomalous Diffusion in Heterogeneous Porous Media," *J. Stat. Phys., 62* (1991), 415–424.

[16] Graham, W. and McLaughlin, D., "Stochastic Analysis of Nonstationary Subsurface Solute Transport, 1. Unconditional Moments," *Water Resour. Res., 25* (1989), 215-232.

[17] Gray, W. G., and O'Neill, K., "On the General Equations for Flow in Porous Media and Their Reduction to Darcy's Law," *Water Resour. Res., 12* (1976), 148–154.

[18] Haldorsen, H. H., Brand, P. J., and Macdonald, C. J., "Review of the Stochastic Nature of Reservoirs," *Mathematics in Oil Production*, S. Edwards and P. R. King, eds., Clarendon Press, Oxford, 1988, pp. 109–209.

[19] King, P. R., "The Use of Renormalisation for Calculating Effective Permeability," *Transport in Porous Media, 4* (1989), 37.

[20] Mapa, R., Illangasekare, T. H., and Garcia, J., "Upscaling of Water Flow and Solute Transport in Saturated Porous Media: Theory, Computation and Experiments," Progress Report submitted to U.S. Army Waterways Experiment Station, Nov. 1994.

[21] Neuman, S. P., Winter, C. L., and Newman, C. M., "Stochastic Theory of Field-Scale Fickian Dispersion in Anisotropic Porous Media," *Water Resour. Res., 23* (1987), 453–466.

[22] Neuman, S. P., Zhang, Y. K., and Levin, O., "Quasilinear Analysis, Universal Scaling, and Lagrangian Simulation of Dispersion in Complex Geological Media," *Dynamics of Fluids in Hierarchical Porous Media*, J. H. Cushman, ed., Academic Press, London, 1990, pp. 349–391.

[23] Plumb, O. A., and Whitaker, S., "Diffusion, Adsorption, and Dispersion in Heterogeneous Porous Media: The Method of Large-Scale Averaging," *Dynamics of Fluids in Hierarchical Porous Media*, J. H. Cushman, ed., Academic Press, London, 1990, pp. 149–176.

[24] Rubin, Y., and Gomez-Hernandez, J. J., "A Stochastic Approach to the Problem of Upscaling of Conductivity in Disordered Media: Theory and Unconditional Numerical Simulations," *Water Resour. Res., 26* (1990), 691–701.

[25] Russell, T. F., "Eulerian-Lagrangian Localized Adjoint Methods for Advection Dominated Problems," *Numerical Analysis 1989*, D.F. Griffiths and G.A. Watson, eds., Pitman Research Notes in Mathematics Series, Vol. 228, Longman Scientific and Technical, Harlow, U. K., 1990, pp. 206–228.

[26] Schiegg, H. O., *Laboratory Setup and Results of Experiments on Two-Dimensional Multiphase Flow in Porous Media,* Pacific Northwest Laboratory Report, Oct. 1990.

[27] Wheatcraft, S. W., Sharp, G. A., and Tyler, S. W., "Fluid Flow and Solute Transport in Fractal Heterogeneous Porous Media," *Dynamics of Fluids in Hierarchical Porous Media*, J. H. Cushman, ed., Academic Press, London, 1990, pp. 305–326.

[28] Zhang, Q., "Length Scales, Multi-Fractals and Non-Fickian Diffusion," *Computational Methods in Water Resources IX, Vol. 2: Mathematical Modeling in Water Resources*, T. F. Russell *et al.*, eds., Computational Mechanics Publications, Southampton, U. K., 1992, pp. 59–70.

CENTER FOR COMPUTATIONAL MATHEMATICS REPORTS

University of Colorado at Denver
P.O. Box 173364, Campus Box 170
Denver, CO 80217-3364

Fax: (303) 556-8550
Phone: (303) 556-8442
http://www-math.cudenver.edu/

58. J.R. Lundgren and S.K. Merz, "Elimination Ordering Characterizations of Digraphs with Interval and Chordal Competition Graphs."
59. H.J. Greenberg, "A Bibliography for the Development of An Intelligent Mathematical Programming System."
60. H.J. Greenberg, "The ANALYZE Rulebase for Supporting LP Analysis."
61. J. Mandel, R. Tezaur and C. Farhat, "An Optimal Lagrange Multiplier Based Domain Decomposition Method for Plate Bending Problems."
62. P. Le Tallec, J. Mandel and M. Vidrascu, "A Neumann-Neumann Domain Decomposition Algorithm for Solving Plate and Shell Problems."
63. C. Liu, C. Liao, Z. Liu, X. Zheng and S. McCormick, "Multilevel Adaptive Methods for Turbulent Combustion with Detailed Chemistry: Part I."
64. C. Liu, C. Liao, Z. Liu, X. Zheng and S. McCormick, "Multilevel Adaptive Methods for Turbulent Combustion with Detailed Chemistry: Part II."
65. L.P. Franca and A. Russo, "Deriving Upwinding, Mass Lumping and Selective Reduced Integration by Residual-Free Bubbles."
66. J.H. Bramble, A.V. Knyazev and Joseph E. Pasciak, "A Subspace Preconditioning Algorithm For Eigenvector/Eigenvalue Computation."
67. S.C. Billups, S.P. Dirkse and M.C. Ferris, "A Comparison of Algorithms for Large Scale Mixed Complementarity Problems."
68. P. Vaněk, R. Tezaur, M. Brezina and J. Křížková, "Two-level Method with Coarse Space Size Independent Convergence."
69. P. Vaněk and S. Ghosal, "A New Technique for Construction of Image Pyramids."
70. L.P. Franca and A. Russo, "Mass Lumping Emanating from Residual-Free Bubbles."
71. L.P. Franca and A. Russo, "Unlocking with Residual-Free Bubbles."
72. C. Liu, Z. Liu and G. Xiong, "Direct Numerical Simulation for the Receptivity and the Whole Process of Transition Around 2-D Airfoils."
73. R. Tezaur, P. Vaněk and M. Brezina, "Two-Level Method for Solids on Unstructured Meshes."